Supplemental Material:

Adjustable Diffusion Enhancement of Water Molecules in a Nanoscale Water Bridge

Yangchao Lu[1, 3], Jige Chen[1, 2]

[1]*Shanghai Institute of Applied Physics, Chinese Academy of Sciences, Shanghai 201800, China*

[2]*Shanghai Synchrotron Radiation Facility, Zhangjiang Laboratory, Shanghai Advanced Research Institute, Chinese Academy of Sciences, Shanghai 201210, China*

[3]*University of Chinese Academy of Sciences, Beijing 100049, China*

PS1. Pressure Variation in the Two Water Reservoirs

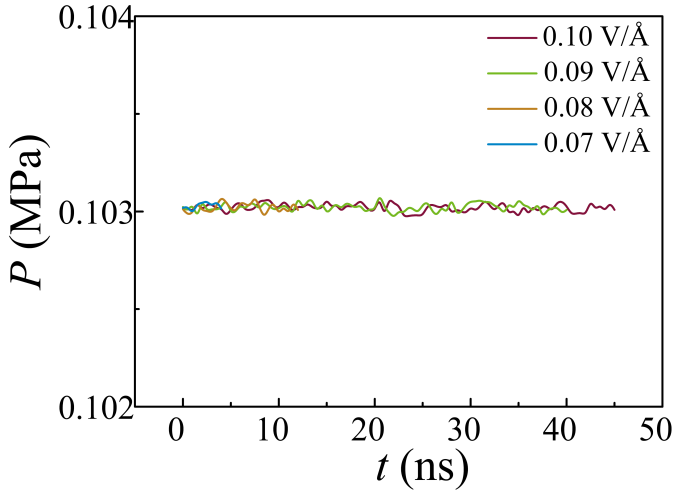

Fig. S1 Time variations of the average pressure of the water molecules in the two water reservoirs when E_Z =0.07, 0.08, 0.09,0.10 V/ Å.

The MD simulations are carried out in an NPT ensemble with T=300 K and P=0.1 MPa. The constant pressure is maintained externally by adding two pressurized walls at the end of the two reservoirs. As illustrated in Fig. 1(a), the water environment is confined between two graphene plates and the external pressure is realized by adding a constant force upon the atoms of the left and right graphene plates. The graphene

plates are set as an impermeable self-adjusting walls that are implemented with P=0.1 MPa. The Nosé-Hoover thermal bath is implemented with T=300 K by excluding the two walls.

As shown in Fig. S1, we illustrate the time variations of the average pressure in the two water reservoirs under different external electric field. It shows that, in our simulation timescale, the averaged pressure maintains at a high accuracy value as the one implemented by the pressured walls. For the electric field E_Z =0.07, 0.08, 0.09,0.10 V/ Å, the averaged pressure P=0.1 MPa is maintained as expected.

PS2. Formation, Stabilization and Breaking of the Water Bridge

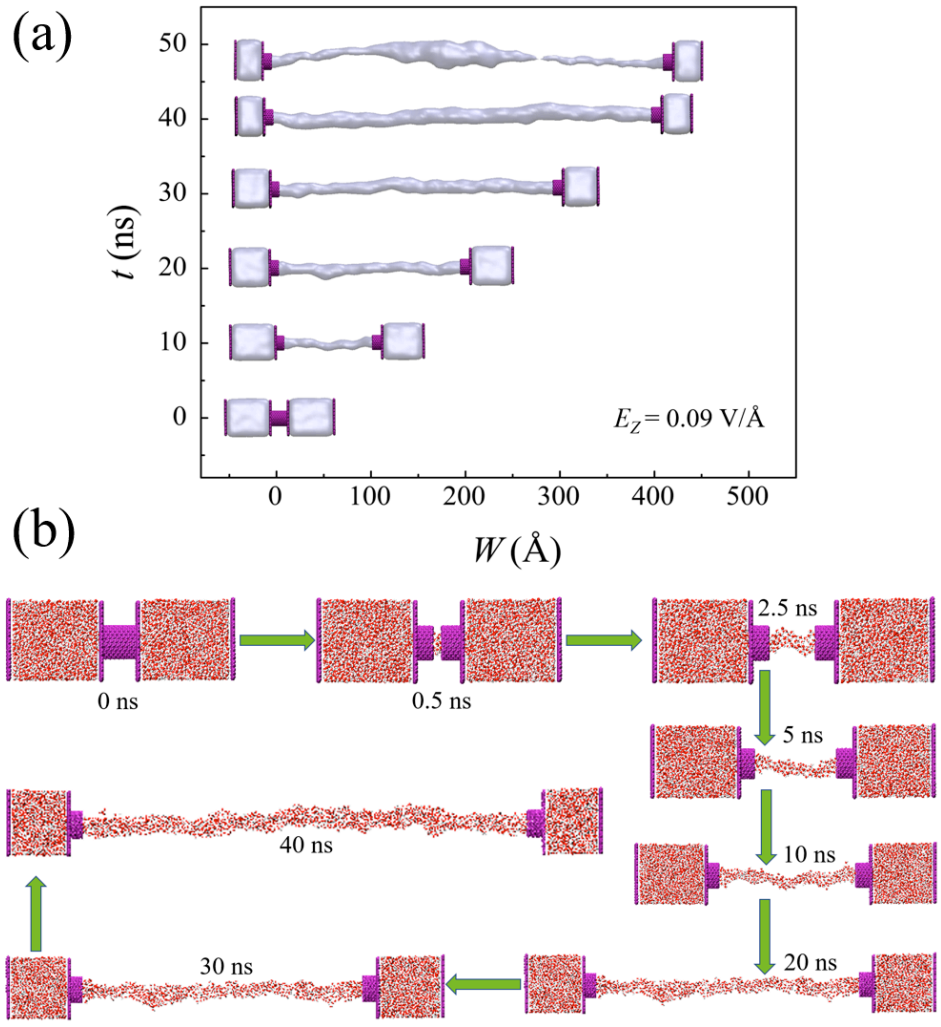

Fig. S2 (a) Snapshots of different water bridge length when the E_Z=0.09 V/Å. y-axis is the simulation time that corresponds to the specific water bridge length. (b) Snapshots of water bridge at different simulation time when the E_Z=0.09 V/Å.

Under the external electric field applied in the z-axis direction, water molecules would fill up the gap between the two disjoint nanotubes as a nanoscale water bridge. The water bridge would stretch itself by increasing the length between the two disjoint CNTs. As a typical example, in Fig. S2(a), we show the snapshots of different water bridge length when the electric field E_Z =0.09 V/Å. The two disjoint CNTs are separated with a constant velocity 1 m/s. The water bridge would stretch itself to sustain the suspended water channel to connect the two disjoint CNTs. As discussed in Fig. 3 in the manuscript, the density and surface tension of the water bridge would increase with its length. The water bridge would break at the final stage at the middle where the highest surface tension is observed when the restrained reordering from the external electric field cannot sustain the increased surface tension.

The formation and breaking process of the water bridge is also illustrated in the supplementary movie S1. Furthermore, we also provide supplementary movies of the water bridge at equilibrium with and without the electric field. Movie S2 and S3 refer to the equilibrium MD simulations of a water bridge with length L=40.0 nm and the E_Z=0.09 V/Å. Movie S4 refers to the water bridge with length L=1.5 nm and the E_Z=0.0 V/Å (without electric field, as a comparison).

PS3. Structural Characteristics of the Water Bridge

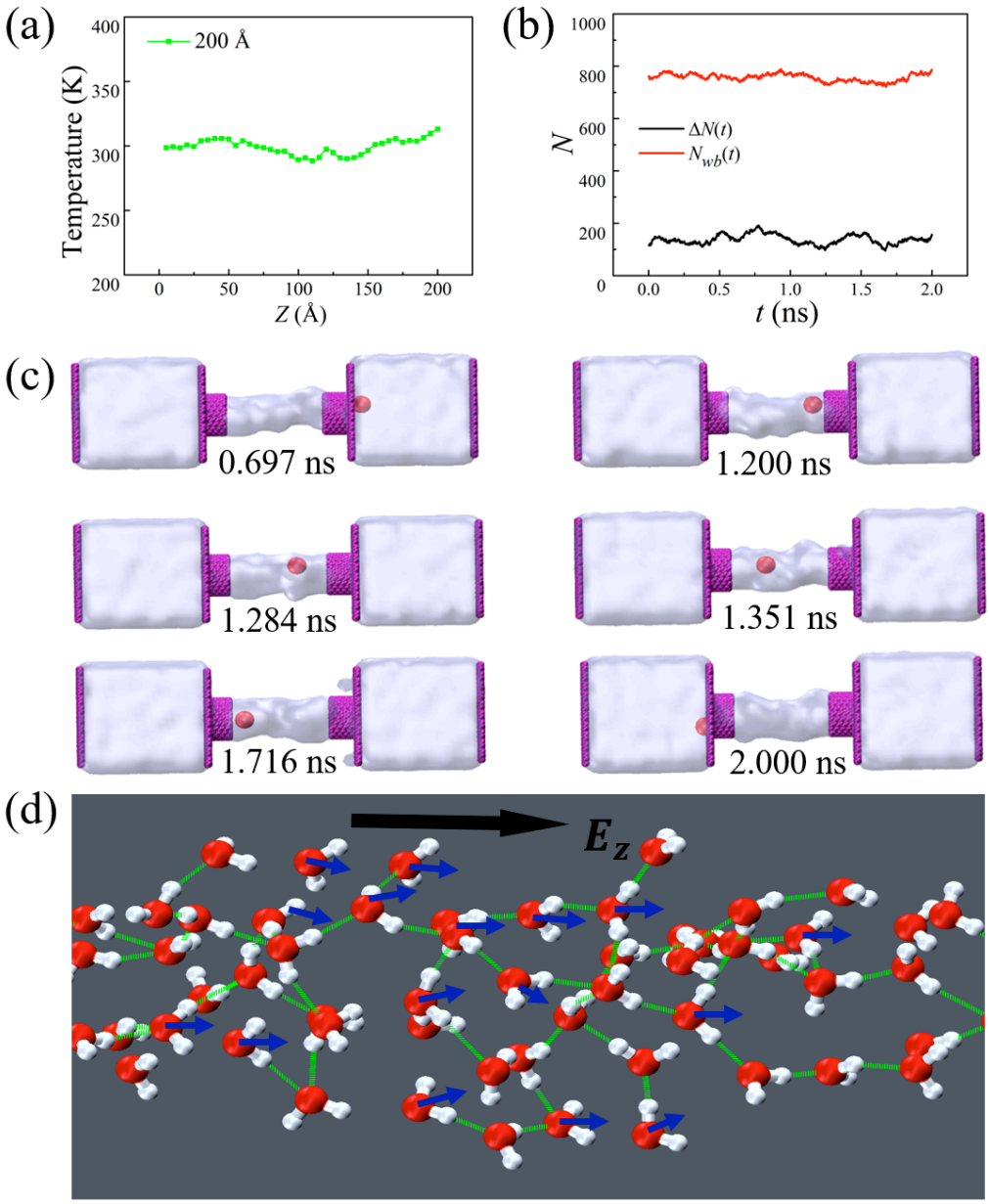

Fig. S3 (a) Temperature distribution along the water bridge. (b) Time variations of the number of the water molecules in the water bridge and number difference of the water molecules between two reservoirs. As a typical example, the temperature distribution and the time variance of the number of the water molecules were calculated from the specific water bridge length L=200 Å when E_Z=0.09 V/Å. (c) Snapshots of the diffusion process for one water molecule from one water reservoir to the other one. Here L=40 Å and E_z=0.09 V/Å. Purple sheets represent carbon atoms and red spheres

represent the target water molecule. (d) Typical snapshot of the dipole moment and hydrogen bonds of the water molecules in the water bridge where L=100 Å and E_z=0.09 V/Å. The blue lines denote the dipole moments of the water molecules and the green lines denote the hydrogen bonds of the water molecules.

By using an electric field, water molecules connect two separate disjoint nanotubes and form a nanoscale water bridge. But will the water bridge hold steady at a specific length and what's the structural characteristics of the water bridge? To investigate this question, the system is fixed at a specific water bridge length and run for another 2ns. Then we calculated the temperature distribution of the water bridge and water molecule number in the water bridge. As a typical example, the data was calculated from the specific water bridge length L=200 Å with E_Z=0.09 V/Å. Fig. S3 (a) shows the temperature distribution along the water bridge. The results show that, temperature along the water bridge at different positions could be considered as identical within the statistical inaccuracy of the MD simulations.

We also calculated the number of water molecules in the water bridge and the number difference of the water molecules between two water reservoirs. The results indicate that no net water flux occurs. We defined a net water flux as,

$$\Delta N(t)=N_1(t)-N_2(t) \quad (1)$$

where $N_1(t)$ is the number of the water molecules in the left water reservoir and $N_2(t)$ is the number of the water molecules in the right water reservoir. As shown in Fig. S3 (b), $\Delta N(t)$ fluctuates around a steady value and no tendency of increase or decrease is observed. Therefore, no net water flux occurs in this equilibrium state.

Water molecules are able to diffuse from one water reservoir to another. The typical transport trajectories of a water molecule diffusing from one water reservoir to another within 1.3 ns are illustrated in Fig. S3(c).

The order parameter provides a statistical measure of the average dipole orientation of the water molecules in the water bridge. The average number of hydrogen bonds provides a statistical measure of the hydrogen bond formation of the water molecules in the water bridge. To illustrate the dipole orientation of the water molecules directly, we also provide a typical snapshot of the dipole moment and the hydrogen bonds. As shown in Fig. S3(d), water molecules exhibit a preferential dipole orientation and form hydrogen bonds along the direction of the electric field.

PS4. MSD Calculations of the Water Molecules

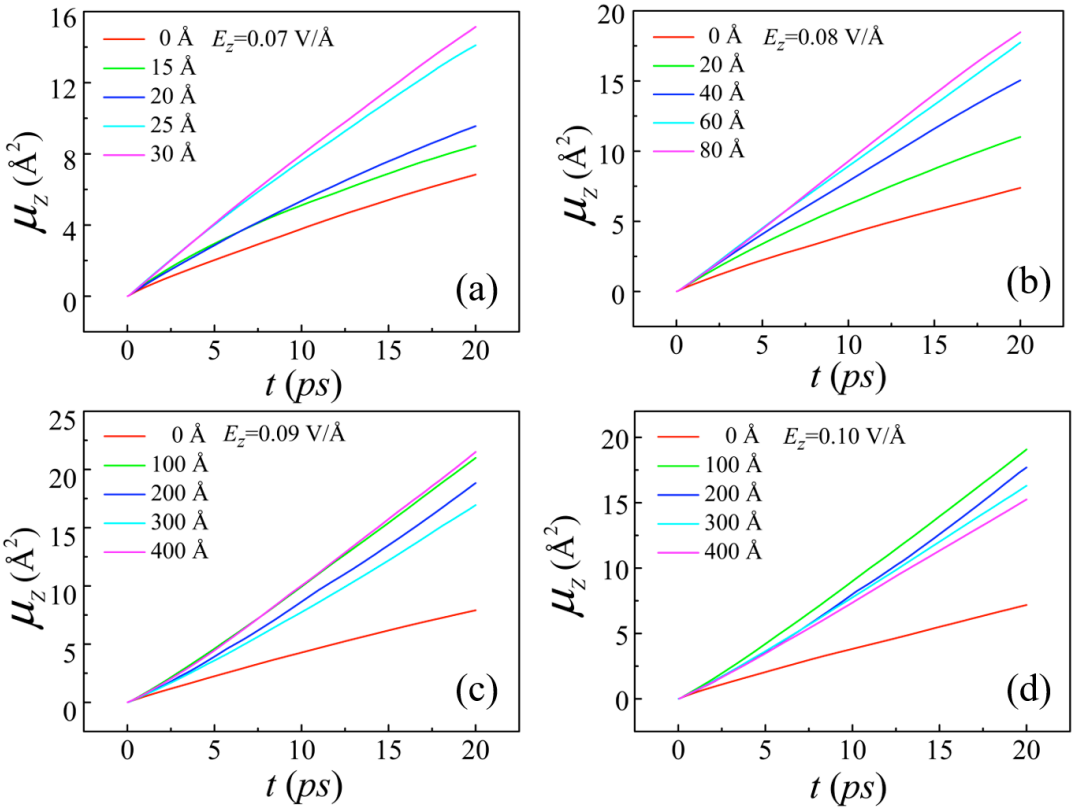

Fig. S4 MSDs of the water bridge under different external electric field. Here we take 5 characteristic MSDs as typical examples.

To investigate the diffuse process of the water bridge molecules, the system is fixed at a specific water bridge length and run for another 2ns. During the simulated time, the system is equilibrium as the Fig. S3 has proved. To calculate the mean square displacement variations (MSD) of the water molecules, four different simulations from different initial conditions are concerned to get the averaged value. Here 5 MSD variations $\mu_Z(t)$ are illustrated as typical examples to represent the diffusion variations of the water molecules in the water bridge.

The diffusion coefficients could be derived as,

$$D_Z = \frac{1}{2N_D \mathrm{d}t}\mu_Z(t) = \frac{1}{2N_D dt}\frac{1}{N_o}\sum_{i=1}^{N_o}[r_{Zi}(t) - r_{Zi}(0)]^2 \qquad (2)$$

where N_D is the dimensionality of the system and $r_{Zi}(t)$ is the position of oxygen atom of the ith water molecule along z-axis at time t, and N_O is the number of oxygen atom in the water bridge. As shown in Fig. S4, the MSD variations of $\mu_Z(t)$ exhibit an excellent linear dependence upon time t, which perfectly fulfills the Einstein relation. Therefore, this result implies that ensemble averages are well within the MD inaccuracy to estimate the diffusion coefficients of the water molecules.

PS5. Effect of the Strong Electric Field on the Water Bridge Formation

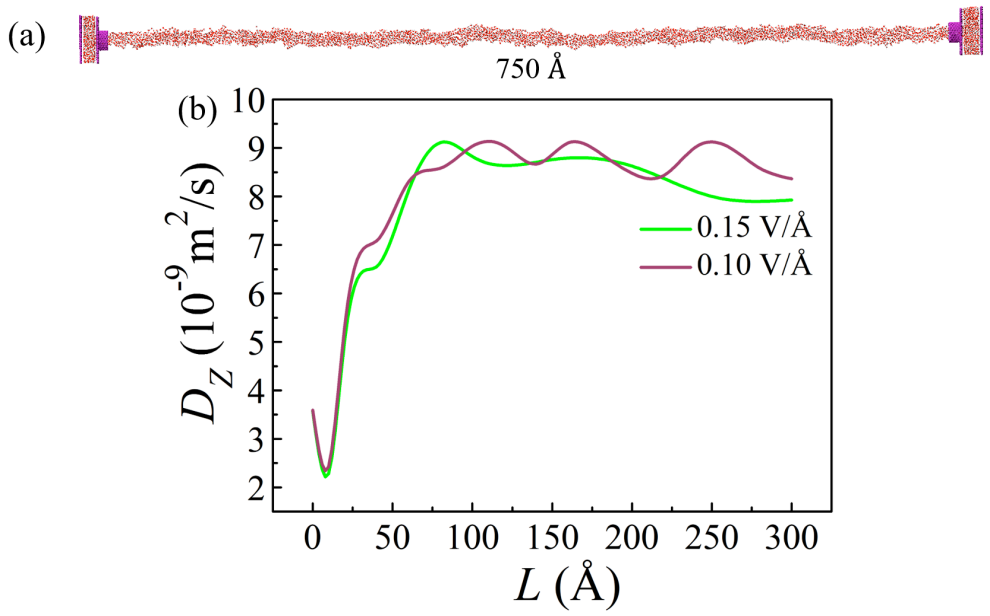

Fig. S5 (a) A snapshot of the water bridge L=750 Å with E_z=0.15 V/Å. (b) Diffusion coefficient of the water bridge molecules in specific water bridge length with E_z=0.10 V/Å (dark red line) and E_z=0.15 V/Å (green line).

To investigate the effect of a large electric field on the formation of the water bridge, we add several new MD simulations by using E_z=0.15 V/Å. As shown in Fig. S5(a), a 750 Å water bridge forms across the two water reservoirs. Particularly, the water bridge will not break even the two water reservoirs are almost empty. The diffusion coefficients of the water bridge molecules with specific bridge length are also calculated. As shown in Fig. S5 (b), when E_z=0.15 V/Å, D_z exhibits similar value as by using E_z=0.10 V/Å. The result is consistent with the simulation results in the manuscript, where a stronger electric field indicates a longer maximum length of the water bridge. The diffusion coefficients of the water molecules rely on the specific length of the water bridge rather than the strength of the eclectic field.

PS6. Effect of Water Models on the Water Bridge Formation

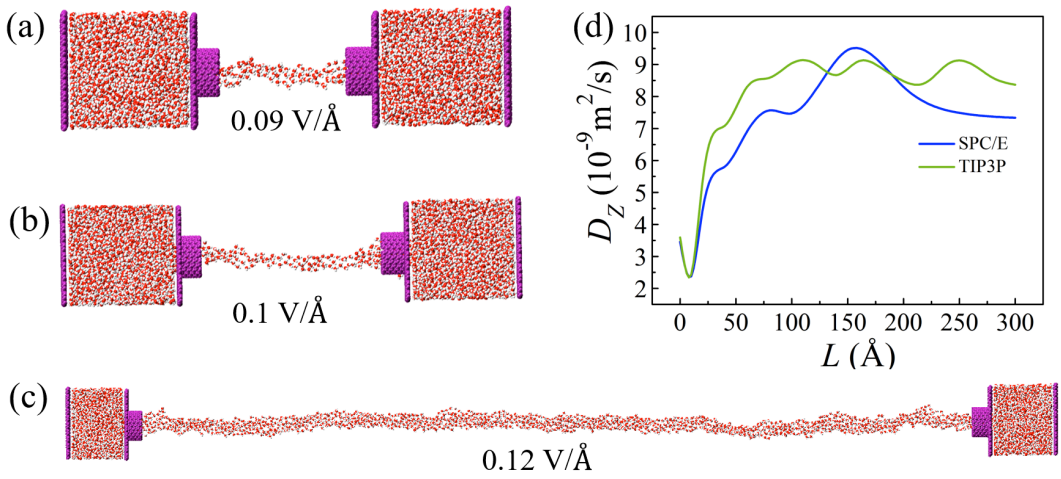

Fig. S6 (a) (b) (c) Snapshots of the water bridges with SPC/E water model with E_z=0.09 V/Å, E_z=0.10 V/Å, E_z=0.12 V/Å. (d) Diffusion coefficient compare of the different kind of water bridge molecules in specific water bridge length. The blue line is the diffusion coefficient of the SPC/E water model with E_z=0.12 V/Å. The cyan line is diffusion coefficient of the TIP3P water model with E_z=0.15 V/Å.

To investigate the effect of the different water models on the properties of the water bridge, we use another common water model, i. e., the SPC/E water model. Similar results are observed by using the SPC/E water model, where a water bridge is formed under the external electric field and the enhanced diffusion coefficient is obtained. As shown in Fig. S6(a)-(c), the snapshots of the water bridges by using the SPC/E water model under electric field with E_z=0.09 V/Å, E_z=0.10 V/Å, E_z =0.12 V/Å around 50 Å, 90 Å, 500 Å respectively. On the other hand, to maintain a steady long water bridge (L> 300 Å), a stronger electric field such as E_z =0.12 V/Å is needed. The diffusion coefficients of the water molecules in the water bridge are similar by using the SPC/E

water model. As shown in Fig. S6(d), a similar enhancement tendency is obtained by using the SPC/E water model.

PS7. Influence of the CNT Diameter upon the Water Bridge Formation

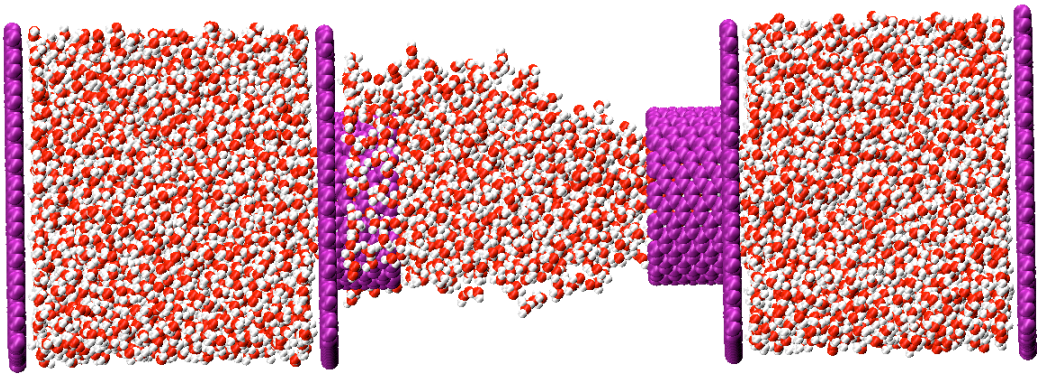

Fig. S7 Snapshot of the water bridge formation between two disjoint (16,16) nanotubes.

The influence of CNT diameter upon the water bridge formation is also investigated. We use two disjoint (16,16) nanotubes (their diameters are about 21.7 Å) and the same water reservoirs to study the water bridge formation under E_z=0.09 V/Å. As shown in Fig. S7, a water bridge forms between the two large CNTs with L=40 Å. On the other hand, since the diameter is increased, more water molecules tend to leak out the nanotubes and it is difficult to maintain a long water bridge due to the increased diameter. Similar results are also observed in literatures (J. Chem. Phys. 143, 094702 (2015), Nanomaterials, 10, 736 (2020)) where the formation of a water column is dependent upon the diameter of nanopores between two graphene plates.[2, 3]

PS8. Effect of the Surface Functionalization on the Water Bridge Formation

It is noteworthy that structure such as surface functionalization would change the structure and dynamics of the water bridge. Adding surface charges is one of the most common theoretical models to study the effect of functionalization to the transport behavior of water inside nanotubes. Here, we use two typical charge patterns on the nanotube surface to investigate the effect of surface functionalization. Similar charge patterns are observed in Carboxyl-Terminated SAM surfaces and hydroxylated SiO2 substrate, and used for one-step reduction and decoration of graphene oxide with gold nanoparticles (NAuNPs) to form a gold-nanoparticles-reduced graphene oxide (NAu-rGO) nanocomposites, hydrothermally synthesized hybrid structure of NiS2-rGO and CoS-rGO nanocomposite.[4-7]

As shown in Fig. S8(b) and (c), similar water bridge formation is observed between the surface charged nanotubes. The adjacent charge pattern (pattern A) can form a 110 Å long water bridge and the barred charge pattern (pattern B) can form a 70 Å long water bridge when the electric field E_z=0.09 V/Å. Comparing with the original system where the maximum length of the water bridge is more than 400 Å, surface charges on the nanotubes exhibit negative effect upon the stability of the water bridge. It is due to the fact that surface charges indicate stronger interactions from the nanotube and thus it is against the hydrogen bond formation in the water bridge. Meanwhile, as discussed in literature[8], due to its hexagonal structure, the barred charge pattern (pattern B) exhibits stronger interactions upon the water molecules and breaks their hydrogen bond connections. As a result, it leads to almost halved water bridge length (70 Å) by comparing with the adjacent charge patterned nanotubes (110 Å).

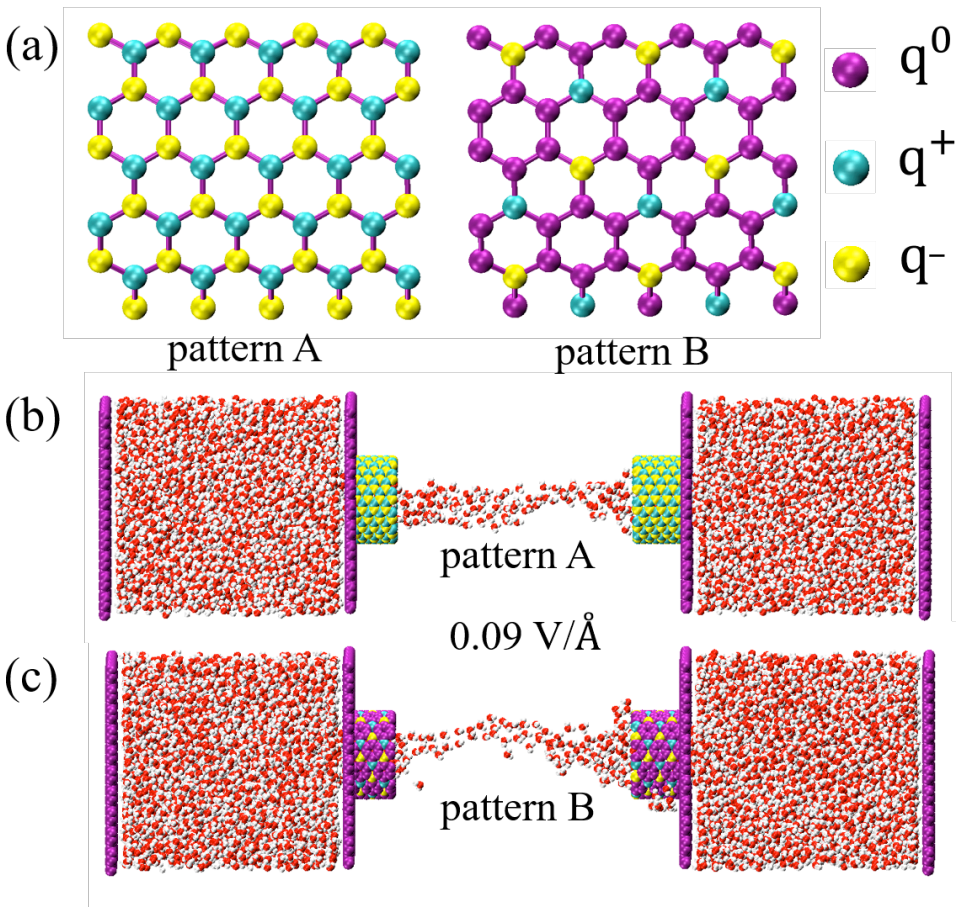

Fig. S8 (a) Geometry of the charge patterns in the nanotubes, where q0 represents the non-charged atoms, q+ represents the positive charged atoms, and q- represents the negative charged atoms. The positive and negative charges are placed in adjacent pairs in the hexagonal lattice in the adjacent charge pattern (pattern A), while placed in barred pairs in the barred charge pattern (pattern B). (b) A snapshot of the pattern A system. (c) A snapshot of the pattern B system.

PS9. Effect of Ions on the Water Bridge Formation

To investigate the effect of the ions on water bridge formation, we used 1.25mol/L and 2.5mol/L NaCl solution to replace the pure water. This simulation results verified the inhibiting effect salt solution in water bridge formation.

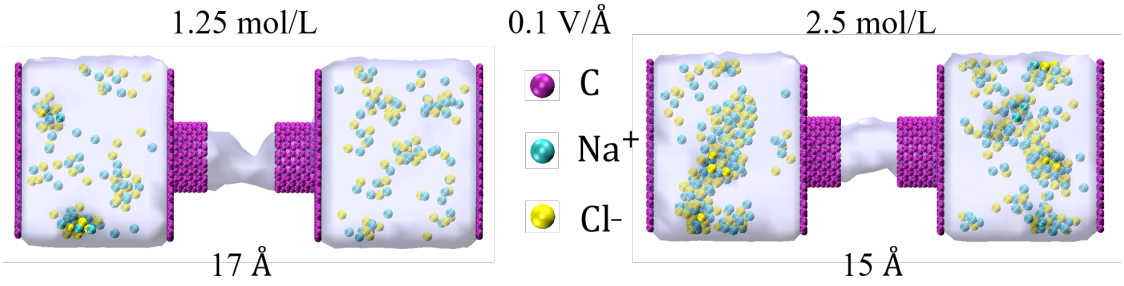

Fig. S9 Snapshot of the 1.25mol/L NaCl and 2.5mol/L NaCl systems. The purple, cyan and yellow spheres represent the carbon atoms, Na^+ and Cl^-, respectively.

As shown in Fig. S9, in the E_z=0.10 V/Å and 1.25mol/L NaCl system, the maximum water bridge length is about L=17 Å. In the E_z=0.10 V/Å and 2. 5mol/L NaCl system, the maximum water bridge length is even less to be L=15 Å. On the other hand, in the pure water system, the maximum water bridge length exceeds 600 Å. It indicates that ions take a strong negative effect upon the water bridge formation. The result is also consistent with experimental observation where the water bridge could be formed in the desalted water. It is particular useful to testify the validity of water desalination devices where a long water bridge is possible with almost pure water.[9]

REFERENCES

1. C. Huang, K. Nandakumar, P. Y. K. Choi and L. W. Kostiuk, *J. Chem. Phys.*, 2006, **124,** 234701.
2. A. Hens, G. Biswas and S. De, *J. Chem. Phys.*, 2015, **143,** 094702.
3. D. L. a. W. Z. Chenchao Li, *Nanomaterials*, 2020, **736,** 094702.
4. P. Guo, Y. S. Tu, J. R. Yang, C. L. Wang, N. Sheng and H. P. Fang, *Phys. Rev. Let.*, 2015, **115,** 186101.
5. X. Nie, J. Chen, N. Sheng, L. Zeng, H. Yang and C. Wang, *Mol. Simul.*, 2017, **43**, 1377.
6. B. Zapotoczny, K. Szafranska, K. Owczarczyk, E. Kus, S. Chlopicki and M. Szymonski, *Sci. Rep.*, 2017, **7,** 7994.
7. P. Borthakur and M. R. Das, *J. Colloid Interf. Sci.*, 2018, **516**, 342.

8. R. Zhang, G. Du, M. Wang, W. Yu and J. Chen, *J. Stat. Mech.*, 2019, **2019**, 063210.
9. J. Liu, G. Shi, P. Guo, J. Yang and H. Fang, *Phys. Rev. Lett.*, 2015, **115,** 164502.